



OPEN

Novel multiferroicity in GdMnO₃ thin films with self-assembled nano-twinning domains

SUBJECT AREAS:
MAGNETIC PROPERTIES
AND MATERIALS
APPLIED PHYSICSXiang Li¹, Chengliang Lu², Jiyan Dai³, Shuai Dong⁴, Yan Chen³, Ni Hu⁵, Guangheng Wu¹, Meifeng Liu¹, Zhibo Yan¹ & Jun-Ming Liu^{1,6}Received
11 August 2014Accepted
23 October 2014Published
12 November 2014Correspondence and
requests for materials
should be addressed to
C.L.L. (cllu@mail.hust.
edu.cn) or J.-M.L.
(liujm@nju.edu.cn)

¹Laboratory of Solid State Microstructures and Innovation Center of Advanced Microstructures, Nanjing University, Nanjing 210093, China, ²School of Physics, Huazhong University of Science and Technology, Wuhan 430074, China, ³Department of Applied Physics, Hongkong Polytechnic University, Hongkong, China, ⁴Department of Physics, Southeast University, Nanjing 211189, China, ⁵Department of Physics, Hubei University of Technology, Wuhan 430068, China, ⁶Institute for Quantum Materials, Hubei Polytechnic University, Huangshi 435000, China.

There have been many interests in exploring multiferroic materials with superior ferroelectric and magnetic properties for the purpose of developing multifunctional devices. Fabrication of thin films plays an important role in achieving this purpose, since the multiferroicity can be tuned via strain, dimensionality, and size effect, without varying the chemical composition. Here, we report exotic multiferroic behaviors, including high- T_C (~ 75 K) ferroelectric state, a large spontaneous polarization ($\sim 4900 \mu\text{C}/\text{m}^2$) and relatively strong ferromagnetism emerging at ~ 105 K, in orthorhombic GdMnO₃/SrTiO₃ (001) thin films with self-assembled nano-scale twin-like domains. We propose a possible *ab*-plane spiral-spin-order phase to be responsible for the large spontaneous polarization in the films, which can only be stabilized by relatively high magnetic field $H > 6$ T in the bulk crystals. It is suggested that the nano-scale twin-like domain structure is essential for the high temperature ferroelectricity and ferromagnetism of the thin films.

Multiferroic materials with coexisting and coupled ferroelectric and magnetic orders, have drawn intensive interests due to their vast application potential and fundamental significance since the first discovery of multiferroicity and giant magnetoelectric (ME) coupling in BiFeO₃ (BFO) and TbMnO₃ (TMO) in 2003^{1–3}. Substantial experimental and theoretical efforts have found a variety of novel multiferroic phases such as the spiral-spin-order (SSO) in (Tb,Dy)MnO₃⁴, E-type antiferromagnetic (AFM) phase in HoMnO₃^{5,6}, spin-dependent *p-d* hybridization induced ferroelectricity in Ba₂CoGe₂O₇⁷, di-atomic Ising spin chains in Ca₃CoMnO₆⁸, possible stripe multiferroic phase in quarter-doped manganites⁹, etc. Although fascinating physics, such as the concurrent time and spatial inverse symmetry breaking, has been revealed, the small ferroelectric (FE) polarizations (P) ($\sim 10^2 \mu\text{C}/\text{m}^2$), the AFM nature, and the low Curie temperatures for FE transitions (T_C) (~ 20 K) keep these materials still far from technological applications.

Recently, quite a few works aiming to explore additional multiferroic materials with excellent physical properties, reported giant improper ferroelectricity ($P = 2900 \mu\text{C}/\text{m}^2$ and $T_C = 90$ K) in the so-called “ferroaxial” magnet CaMn₇O₁₂^{10,11}, and gigantic magnetic field induced FE polarization ($\Delta P = 17000 \mu\text{C}/\text{m}^2$ and $T_C = 64$ K) in ferrimagnetic oxide CaBaCo₄O₇¹². Some earlier studies revealed above room temperature multiferroic states and low magnetic field induced ME effect in hexaferrites, although their FE polarizations are still small¹³. These exciting results point to a promising future of multiferroics for the fabrication of multifunctional devices near room temperature. Meanwhile, recently the way to explore novel multiferroicity by finely tuning the multiple exchange interactions in these classic multiferroic materials has been confirmed to be efficient too. Giant tunability of the FE polarization ($\Delta P = 5000 \mu\text{C}/\text{m}^2$) through modifying the Gd-Mn symmetric exchange striction by magnetic field was reported in GdMn₂O₅¹⁴. Interesting strain engineered ferromagnetic (FM) tendency was widely probed in multiferroic manganite (TbMnO₃, YMnO₃, and LuMnO₃) thin films^{15–19}. In particular, while the corresponding bulk crystal are well known as a robust antiferromagnet, a clear FM hysteresis loop and a large ferromagnetism ($\sim 1.0 \mu_B$) were captured in the orthorhombic LuMnO₃ thin film by polarized neutron reflectometry¹⁹. Additionally, remarkable FE polarization ($\sim 12 \mu\text{C}/\text{cm}^2$) was theoretically predicted in highly compressively strained HoMnO₃ thin films²⁰, which is already comparable with that of traditional ferroelectric oxides such as BaTiO₃²¹.



For the strain effect in thin films, one of the most direct consequences is the modified microstructure due to lattice misfit between the films and substrates. This misfit would modulate the physical properties massively. One typical example is the multiferroic $\text{YMnO}_3/\text{SrTiO}_3$ (STO) thin films, in which the ground state can be changed from E-AFM to SSO by strain corresponding to the reduced orthorhombicity of the films²². Another example is BiFeO_3 which shows similar SSO phase in the bulk crystals, while this non-collinear spin state can be easily replaced with a collinear spin order by means of strain engineering (no matter compressive or tensile) in thin films²³. In addition to the modified microstructure, the electron-lattice coupling due to the Jahn-Teller (JT) distortion could also be appreciable to physical properties. In HoMnO_3 thin films, it was predicted that the strain tuned electron-lattice coupling could induce a progressive electronic contribution to the FE polarization²⁰, although it still needs to be examined experimentally. Here one interesting feature is worth mentioning that the nano-scale twin-like domains are formed naturally to reduce the strain energy in multiferroic $\text{RMnO}_3/\text{SrTiO}_3$ thin films^{17,18}. This multi-domain structure, in addition to the electron-lattice coupling tuning, was proposed to be responsible for the ferromagnetic tendency in RMnO_3 thin films^{17,18}, while its possible impact on the magnetically driven ferroelectricity is so far not clear.

In the present work, we report remarkably enhanced spontaneous electric polarization along the a -axis, $P_a \sim 4900 \mu\text{C}/\text{m}^2$, high ferroelectric phase transition temperature $T_C = 75 \text{ K}$, and weak ferromagnetism emerging at $T \sim 105 \text{ K}$ in modestly strained GdMnO_3 (GMO) thin films grown on (001) STO substrates, while these thin films accommodate nano-scale twin-like domains. These novel multiferroic properties probably can be explained in the framework of strain stabilized ab -plane SSO phase and twin-like domain structure. There are three motivations for choosing GMO. First, the orthorhombic RMnO_3 with small rare-earth element R is a typical multiferroic material, and the multiferroic state shows plentiful variations upon tuning the inherent orthorhombic distortion²⁴. For example, the SSO in TMO and DyMnO_3 (DMO) can be transformed to an E-type AFM state by simply replacing the Tb/Dy with smaller Ho²⁴. On the other side, if the Tb/Dy is substituted by larger rare earth Gd, the situation becomes complicated^{25,26}. GMO locates rightly at the phase boundary between the A-type AFM and ab -SSO, as illustrated in Fig. 1, and a small spontaneous P_a ($\sim 40 \mu\text{C}/\text{m}^2$) arises along the a axis, which could be significantly tuned by disorder or defects²⁵. Importantly, the P_a can be enhanced up to 100 times by strengthening the ab -SSO phase with a magnetic field $H > 6 \text{ T}$ ($P_a \sim 4000 \mu\text{C}/\text{m}^2$ at $H > 6 \text{ T}$ and $E_a = 8 \text{ MV}/\text{m}$), which is the largest value reported so far among the SSO multiferroic manganites²⁴. Considering the high sensitivity of multiferroicity to physical excitations in GMO, it would be possible to stabilize the remarkable P_a by some practically accessible methods such as the strain in thin films instead of high magnetic field. Second, GMO is on the border of A-type AFM phase, which allows an easy access to weak ferromagnetism due to spin-canting induced by the highly distorted crystalline structure^{24,27}. The canted A-AFM with a net ferromagnetic moment M_c is schematically drawn in the top left of Fig. 1. Therefore, it would be interesting to explore the possible coexistence of large spontaneous polarization and ferromagnetism engineered by strain in GMO thin films. Third, according to the earlier studies^{17,18}, we note that the nano-scale domain structure is possible in multiferroic $\text{RMnO}_3/\text{SrTiO}_3$ thin films. We expect similar nano-domains appearing in GMO/STO thin films. Moreover, possible reconstruction of the magnetic ordering due to size effect would be anticipated, which could induce distinct multiferroicity in thin films considering the close relationship between ferroelectric and magnetic orders.

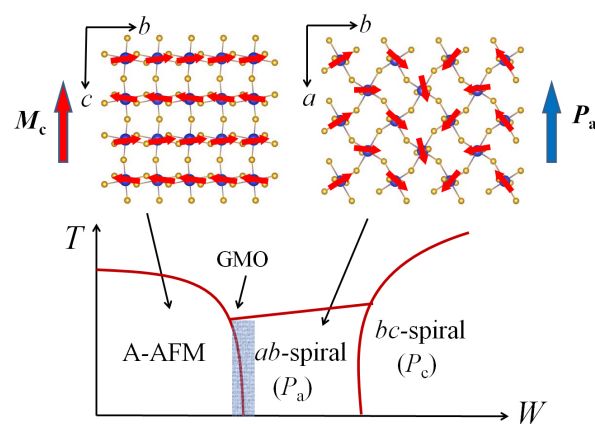


Figure 1 | Schematic drawing of the canted A-type antiferromagnetic phase (left) and ab -plane spiral spin ordering phase (right). Sketch of the magnetic phase diagram which shows the phase evolution with bandwidth W .

Results

Fig. 2(a) displays the high resolution X-ray diffraction (HRXRD) pattern of a typical GMO/STO thin film with thickness $t = 110 \text{ nm}$. The film shows pure phase and single c -axis orientation. The out-of-plane lattice parameter is determined to be $\sim 7.479 \text{ \AA}$ which is slightly larger than the $c \sim 7.431 \text{ \AA}$ for GMO bulk single

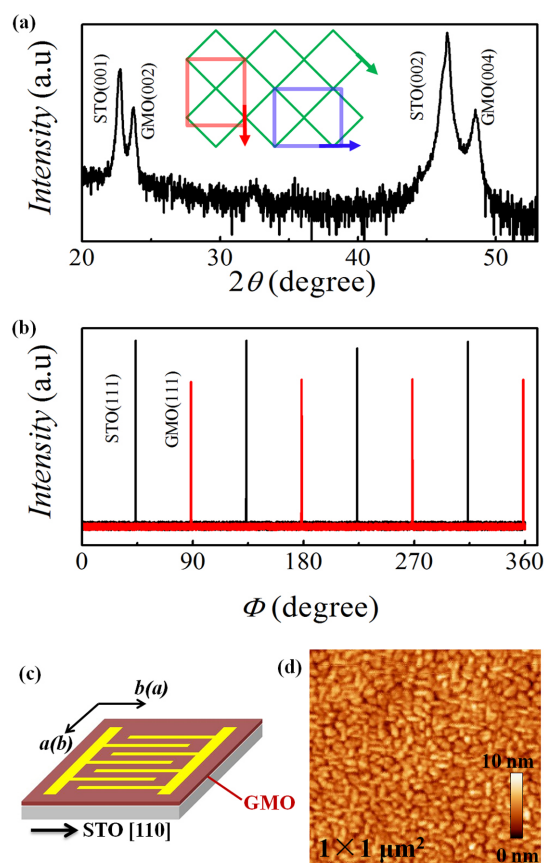


Figure 2 | (a) Typical θ - 2θ scan of $\text{GdMnO}_3/\text{SrTiO}_3$ thin films. The inset shows the epitaxial growth model, where the green squares denote the STO lattice, and the red and blue rectangles denote the twin-like film lattice. The arrows indicate the $[100]$ direction of the film or the substrate. (b) Φ -scan of GdMnO_3 (111) and SrTiO_3 (111) reflections. (c) Sketch of the device structure. (d) Surface morphology of the film.



crystal²⁸, proving a small in-plane compressive strain. To check the epitaxy of the film growth, we further did Φ -scan which is shown in Fig. 2(b). Four GMO (111) peaks with an equal separation of 90° can be seen clearly, which is accompanied by the expected four-fold STO (111) reflections but with a 45° shift. This feature verifies epitaxial growth of the GMO films with respect to the STO substrates. Moreover, the 45° deviation of the GMO (111) peaks as for the STO (111) reflections suggests that the orthorhombic unit cell of GMO is grown on a $3.905\sqrt{2} \text{ \AA} \times 3.905\sqrt{2} \text{ \AA}$ square STO lattice, which can accommodate the in-plane film lattice better. Since the orthorhombic GMO shows strong structural anisotropy with lattice parameters $a = 5.318 \text{ \AA}$, $b = 5.866 \text{ \AA}$, and $c = 7.431 \text{ \AA}$ ²⁸, huge lattice misfit (-3.7% along a axis and 6.2% along b axis) would still be expected intuitively for the epitaxial growth of GMO on the top of STO, which is drastically different from the modest compressive strain as revealed by the XRD data. It is then implied that additional microstructural features appear in order to release these huge in-plane strains, consistent with the quite small variation of the out-of-plane lattice constant c .

In order to capture further details of the film microstructures, plane-view transmission electron microscopy (TEM) measurements were conducted and some typical images are highlighted in Fig. 3. As shown in Fig. 3(a), the film has a nano-scale multi-domain structure, and the mean size of the domains is around 30 nm and relatively uniform. This is consistent with the domain structure observed by atomic force microscopy measurement shown in Fig. 2(d). A closer plane-view TEM image reveals two variants in the film, which are perpendicular to each other as shown in Fig. 3(b). The corresponding electron diffraction pattern shown in Fig. 3(c) confirms this twin-like domain structure. From the high-resolution TEM image shown in Fig. 3(d), some weak fringes can be seen at/near the domain boundaries, suggesting to be the Morie fringes during the overlapping of domains at the boundaries and the rotation with respect to the variants 1 and 2. The observed twin-like domain structure can further reduce the anisotropic strain energy during the epitaxial growth, giving rise to the small compressive strain of the film. Similar twin-like domain structure was reported in other multiferroic RMnO_3 thin films^{15–18,29,30}, which is probably a common feature for the epitaxial growth of such films once the mismatching strain is anisotropic.

The in-plane magnetization (M) as a function of T and H is presented in Fig. 4. Although the GMO bulk crystals show successive magnetic phase transitions^{24–26}, the $M(T)$ curves of the GMO thin film show smooth variation over the whole measured T range, marking modified magnetic properties for the films. Although no evident phase transition can be seen, the $M(T)$ curves of field cooling (FC)

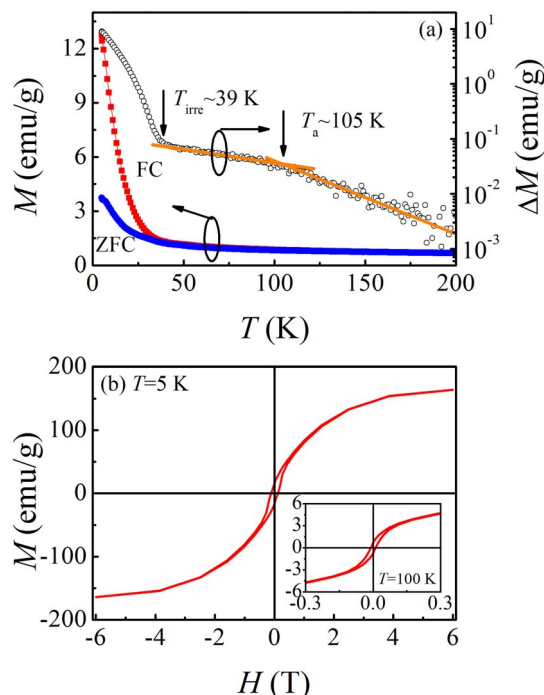


Figure 4 | (a) Temperature dependence of magnetization (magnetic contribution from substrate has been subtracted.) under FC and ZFC cases. The open circles represent the ΔM plotted as a function of T . Two possible phase transitions, T_{irre} and T_a , are indicated by the arrows, respectively. (b) M - H curves measured at $T = 5 \text{ K}$ (the main panel) and $T = 100 \text{ K}$ (the inset).

and zero field cooled (ZFC) cases present noticeable divergence at low T , which is accompanied by a striking increase in M with decreasing T . This feature leads us to argue a possible net magnetization in the GMO thin film. The irreversible temperature is determined to be $T_{\text{irre}} \sim 39 \text{ K}$ by plotting $\Delta M = M_{\text{FC}} - M_{\text{ZFC}}$ as a function of T . The clear magnetic hysteresis loop with coercive field of $H_c = 1.2 \text{ kOe}$ measured at $T = 5 \text{ K}$ confirms the existence of low- T FM phase, as shown in Fig. 4(b). Interestingly, a closer check captures a second anomalous at $T_a \sim 105 \text{ K}$ on the plot of ΔM - T , which signals the onset of long-range magnetic correlation. To probe further, a $M(H)$ curve was measured at 100 K , and a striking FM hysteresis with $H_c = 0.1 \text{ kOe}$ is observed, verifying an exotic FM orders.

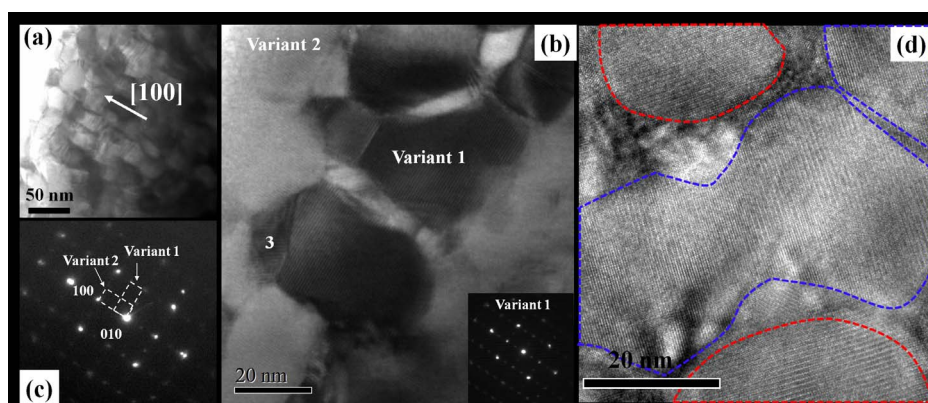


Figure 3 | (a) Plane view transmission electron microscopy image of a 110 nm $\text{GdMnO}_3/\text{SrTiO}_3$ thin film. (b) An enlarged plane view TEM image showing clear twin-like domain structure labeled with ‘variant 1’ and ‘variant 2’. Small region (labeled by 3) shows $\sim 45^\circ$ rotation with respect to the two variants. The inset shows electron diffraction pattern of variant 1. (c) Electron diffraction pattern including both of variant 1 and 2. (d) High resolution TEM image of the same sample. The areas showing different variants are enclosed by blue and red lines, respectively.



The above magnetic data shows significant modulation of the magnetic properties in the GMO thin films as compared to the bulk counterpart, pointing to modified multiferroicity due to the intimate coupling between magnetic and ferroelectric orders in this material. Fig. 5(a) and (b) present the T -dependence of pyroelectric current (I) and corresponding integrated FE polarization, respectively. Surprisingly, a remarkable spontaneous polarization $P_a \sim 4900 \mu\text{C}/\text{m}^2$ along the a -axis of the films is observed (the polarization can never be along the b -axis for both SSO and E-AFM phases in RMnO_3 ³¹). Nearly identical value of P_a (not shown here) was detected along the in-plane perpendicular direction consistent with the above proposed twin-like domain structure. The FE phase transition temperature is derived to be as high as $T = T_C \sim 75 \text{ K}$, which is almost among the highest values for discovered multiferroic materials^{10–13}.

The magnetically driven FE state looks very robust against the magnetic field, and the P_a just shows small variation even the applied field is as large as $H = 9 \text{ T}$. For a comparison, we also measured the I - T curve along the c axis in another sample grown simultaneously, but with a conductive substrate Nb-doped STO (001), as shown in Fig. 5(a). Clearly, no pyroelectric current was found, suggesting the

zero FE polarization along the c -axis of the film. To attest that the measured current along the a -axis do come from the pyroelectricity, we measured the I - T curves for three different heating rates (2–4 K/min) as shown in Fig. 5(a). No evident shift of the peak position of the I - T curves can be seen, suggesting the existence of the FE state. The minuscule move of the peak (less than 1 K) is probably due to the thick substrate (0.5 mm) which prevents quick thermal transport. Moreover, the spontaneous polarization can be reversed by reversing the poling electric field (Fig. 5(b)), and such P_a reversing process can also be realized by switching the electric field isothermally using a PUND method shown in Fig. 5(c). The values of P_a obtained from PUND method are close to that of pyroelectric measurements. These demonstrate once again the FE state in the GMO film.

Discussion

Here, we discuss the possible origins of the large spontaneous ($P_a \sim 4900 \mu\text{C}/\text{m}^2$), high Curie temperature of the FE state, and weak ferromagnetism up to 105 K in GMO/STO thin films. In essence, the observation of spontaneous P_a leads us to argue an ab -spiral spin ordering phase in the thin film similar to the case in GMO bulk crystal, motivated by the magnetic phase diagram of RMnO_3 ^{24,31}. This is further supported by the absence of pyroelectric current along the c -axis (Fig. 5(a)). However, both the onset temperatures of the weak FM phase $T \sim 105 \text{ K}$ and the ferroelectric phase $T_C \sim 75 \text{ K}$ of the film are much higher than that of the bulk, which suggests that the incommensurate AFM temperature ($\sim 40 \text{ K}$) and the SSO temperature ($\sim 8 \text{ K}$) of Mn moments known in bulk DMO have been uniformly moved to high temperature side in the thin films^{24–26}.

First, we look at the high- T phase with weak FM component in the films. Since the films just show very small compressive strain as evidenced by the XRD data, a significant contribution from the lattice modulation by strain is not to be expected. Therefore, we propose that the nano-scale twin-like domain structure is essential for this. This twin-like domain structure is due to the strain relaxation during the epitaxial growth, which has been comprehensively investigated in Ref 18. There are two possible mechanisms responsible for the strain relaxation, which are misfit dislocations at the film-substrate interface and increased strain relaxation at the domain walls. In $\text{LuMnO}_3/\text{YAlO}_3$ thin films which show close lattice misfit ($\Delta c \sim 0.8\%$) to the present case but without twin-like structure, misfit dislocations induced ferromagnetism was demonstrated, while the FM phase can only be observed below 50 K¹⁹. Therefore, more factors should be taken into account for the high- T weak ferromagnetism in the present films. As evidenced by the TEM measurements, the lattice at domain walls shows different arrangement over the domains, which would naturally break the perfect long range AFM orders and thus generate net moment (FM orders) at the domain walls. Actually, surface (assembles the domain walls) ferromagnetism was widely observed in nano-scale perovskite manganites^{32–34}. In particular, similar high temperature anomalous magnetic phase transition at $T \sim 125 \text{ K}$ was observed in TMO/STO thin films which show similar nano-scale domain structure¹⁷.

Second, regarding the FE state with relatively high T_C , the mechanism should be similar to that of the bulk crystals as discussed above. However, this ab -SSO phase is driven to high- T side since the long-range magnetic correlation has been developed in high temperature as evidenced by the magnetic data^{14,24–26,35}. Another possibility is the size effect, owing to the finite size of the domains. It is known that in BiFeO_3 nanoparticle, strong FM tendency could be induced as the particle size is reduced and comes close to the period length of the spiral spin structure³⁶. In the present case, although the ab -SSO period length known in the bulk GMO (few unit cells)²⁶ is shorter than the observed domain size ($\sim 30 \text{ nm}$) in the films, a possible modulation on the period of the SSO phase would still be expected considering its small energy scale (in meV). Therefore, the magnetically driven ferroelectricity would be tuned

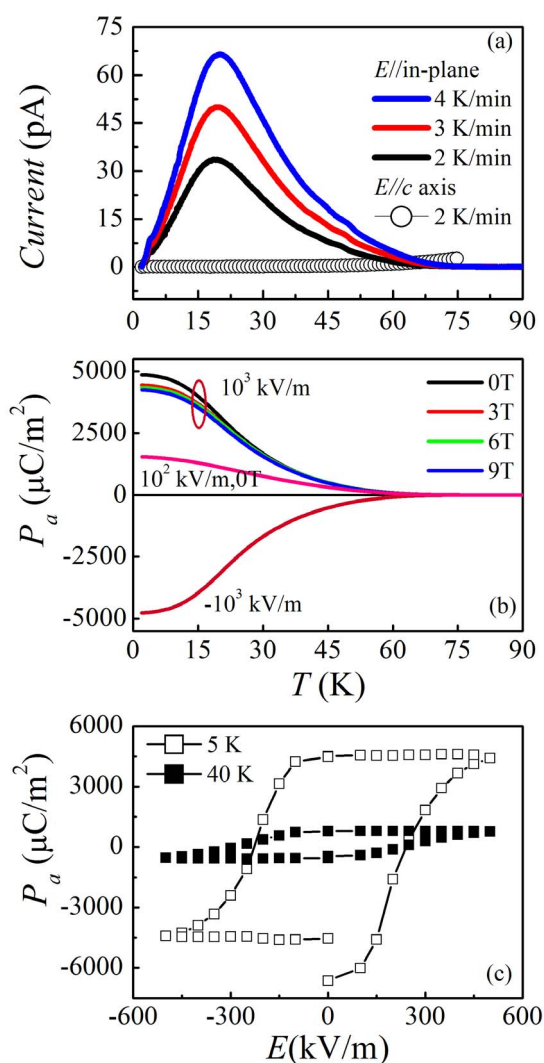


Figure 5 | (a) Pyroelectric current as a function of temperature measured for various heating rates. The circles denote the data measured along c axis. (b) Integrated polarization as a function of temperature under various magnetic fields. (c) Ferroelectric hysteresis loop measured using the PUND method at $T = 5 \text{ K}$ and 40 K .



correspondingly because of the close correlation between SSO period and the related FE properties²².

In a nutshell, multiferroicity of GdMnO₃ thin film grown on SrTiO₃ (001) substrate has been investigated by performing extensive structural, magnetic and ferroelectric measurements. Large spontaneous polarization $P_a \sim 4900 \mu\text{C}/\text{m}^2$ was detected, and a possible *ab*-plane spiral spin ordering phase was proposed to be responsible for it. Interestingly, high ferroelectric phase with $T_C = 75 \text{ K}$ and weak ferromagnetism at $\sim 105 \text{ K}$ were detected, which should be related to the nano-scale twin-like domain structure and strain-modified lattice distortion.

Methods

Sample preparation. Epitaxial GMO thin films with various thickness (*t*) ranging from 10 to 110 nm were grown on STO (001) substrates using pulsed laser deposition (PLD) method. A KrF excimer laser (248 nm wavelength) was used for the deposition with a repetition rate of 3 Hz, and the laser energy density was set at $\sim 1 \text{ J}/\text{cm}^2$. A stoichiometric GMO target was used for the ablation. The depositions were made with substrate temperature of 800 °C and an oxygen partial pressure of 10 Pa. After deposition, the samples were cooled down at 1 atm of oxygen pressure to achieve oxidation.

Structure characterization. High resolution X-ray diffraction analyses were carried out using a Rigaku Rotaflex Diffractometer. Surface morphology of the samples was checked using Bruker Multimode 8 atomic force microscope. The plane-view and cross-section Transmission Electron Microscopy were performed using JEM 2100F microscope.

Ferroelectric and magnetic measurements. In order to probe in-plane ferroelectricity, gold electrodes of an inter-digitated pattern shown in Fig. 2(c) were sputtered on the film surface through standard photolithography and lift-off procedures. The same device structure was used to probe the in-plane ferroelectricity of YMnO₃ thin films early³⁷. The ferroelectric polarization measurements were performed using standard pyroelectric current method using the Keithley 6514 A and 6517 electrometers connected to the Quantum Design Physical Properties Measurement System (PPMS). For each measurement, the sample was first cooled from 150 K to 2 K under a constant poling electric field (*E*). Then, the poling electric field was removed and the sample was short-circuited for sufficient time in order to release any charges accumulated during the poling process. The recorded background current noise amplitude was less than 0.1 pA. The pyroelectric current was collected during the heating process, and various heating rates were used to ensure no contribution other than the pyroelectric current. The polarization was obtained by integrating the collected current with time. To double test the ferroelectricity, PUND method was employed to obtain the *P-E* loops³⁸. Magnetization (*M*) as a function of temperature and magnetic field (*H*) was measured using a Magnetic Properties Measurement System (MPMS, Quantum Design). The cooling and measuring field was set at 0.1 T.

- Kimura, T. *et al.* Magnetic control of ferroelectric polarization. *Nature* **426**, 55 (2003).
- Cheong, S. W. & Mostovoy, M. Multiferroics: a magnetic twist for ferroelectricity. *Nat. Mater.* **6**, 13 (2007).
- Wang, K. F., Liu, J.-M. & Ren, Z. F. Multiferroicity: the coupling between magnetic and polarization orders. *Adv. Phys.* **58**, 321 (2009).
- Tokura, Y. & Seki, S. Multiferroics with Spiral Spin Orders. *Adv. Mater.* **22**, 1554 (2010).
- Picozzi, S., Yamauchi, K., Sanyal, B., Sergienko, I. A. & Dagotto, E. Dual Nature of Improper Ferroelectricity in a Magnetoelectric Multiferroic. *Phys. Rev. Lett.* **99**, 227201 (2007).
- Lee, N. *et al.* Mechanism of exchange striction of ferroelectricity in multiferroic orthorhombic HoMnO₃ single crystals. *Phys. Rev. B* **84**, 020101(R) (2011).
- Murakawa, H. *et al.* Ferroelectricity Induced by Spin-Dependent Metal-Ligand Hybridization in Ba₂CoGe₂O₇. *Phys. Rev. Lett.* **105**, 137202 (2010).
- Choi, Y. J. *et al.* Ferroelectricity in an Ising Chain Magnet. *Phys. Rev. Lett.* **100**, 047601 (2008).
- Dong, S., Yu, R., Liu, J.-M. & Dagotto, E. Striped Multiferroic Phase in Double-Exchange Model for Quarter-Doped Manganites. *Phys. Rev. Lett.* **103**, 107204 (2009).
- Johnson, R. D. *et al.* Giant Improper Ferroelectricity in the Ferroaxial Magnet CaMn₇O₁₂. *Phys. Rev. Lett.* **108**, 067201 (2012).
- Zhang, G. Q. *et al.* Multiferroic properties of CaMn₇O₁₂. *Phys. Rev. B* **84**, 174413 (2011).
- Caignaert, V. *et al.* Gigantic magnetic-field-induced polarization and magnetoelectric coupling in a ferrimagnetic oxide CaBaCo₄O₇. *Phys. Rev. B* **88**, 174403 (2013).
- Wang, F., Zou, T., Yan, L. Q., Liu, Y. & Sun, Y. Low magnetic field reversal of electric polarization in a Y-type hexaferrite. *Appl. Phys. Lett.* **100**, 122901 (2012).

- Lee, N. *et al.* Giant Tunability of Ferroelectric Polarization in GdMn₂O₅. *Phys. Rev. Lett.* **110**, 137203 (2013).
- Marti, X. *et al.* Emergence of ferromagnetism in antiferromagnetic TbMnO₃ by epitaxial strain. *Appl. Phys. Lett.* **96**, 222505 (2010).
- Kirby, B. J. *et al.* Anomalous ferromagnetism in TbMnO₃ thin films. *J. Appl. Phys.* **105**, 07D917 (2009).
- Cui, Y. M., Tian, Y. F., Shan, A. X., Chen, C. P. & Wang, R. M. Magnetic anisotropy and anomalous transitions in TbMnO₃ thin films. *Appl. Phys. Lett.* **101**, 122406 (2012).
- Venkatesan, S., Daumont, C., Kooi, B. J., Noheda, B. & De Hosson, J. T. M. Nanoscale domain evolution in thin films of multiferroic TbMnO₃. *Phys. Rev. B* **80**, 214111 (2009).
- White, J. S. *et al.* Strain-Induced Ferromagnetism in Antiferromagnetic LuMnO₃ Thin Films. *Phys. Rev. Lett.* **111**, 037201 (2013).
- Iusan, D. *et al.* Effects of strain on ferroelectric polarization and magnetism in orthorhombic HoMnO₃. *Phys. Rev. B* **87**, 014403 (2013).
- Choi, K. J. *et al.* Enhancement of Ferroelectricity in Strained BaTiO₃ Thin Films. *Science* **306**, 1005 (2004).
- Villacorta, F. J. *et al.* Strain-driven transition from E-type to A-type magnetic order in YMnO₃ epitaxial films. *Phys. Rev. B* **86**, 024420 (2012).
- Sando, D. *et al.* Crafting the magnonic and spintronic response of BiFeO₃ films by epitaxial strain. *Nat. Mater.* **12**, 641 (2013).
- Kimura, T., Lawes, G., Goto, T., Tokura, Y. & Ramirez, A. P. Magnetoelectric phase diagrams of orthorhombic RMnO₃ (R=Gd, Tb, and Dy). *Phys. Rev. B* **71**, 224425 (2005).
- Lin, L. *et al.* Ferroelectricity of polycrystalline GdMnO₃ and multifold magnetoelectric responses. *Appl. Phys. A* **112**, 947 (2013).
- Feyerherm, R. *et al.* Magnetic-field induced effects on the electric polarization in RMnO₃ (R=Dy, Gd). *Phys. Rev. B* **79**, 134426 (2009).
- Choi, Y. J., Zhang, C. L., Lee, N. & Cheong, S.-W. Cross-Control of Magnetization and Polarization by Electric and Magnetic Fields with Competing Multiferroic and Weak-Ferromagnetic Phases. *Phys. Rev. Lett.* **105**, 097201 (2010).
- Mori, T., Kamegashira, N., Aoki, K., Shishido, T. & Fukuda, T. Crystal growth and crystal structures of the LnMnO₃ perovskites: Ln=Nd, Sm, Eu and Gd. *Mater. Lett.* **54**, 238 (2002).
- Daumont, C. J. M. *et al.* Epitaxial TbMnO₃ thin films on SrTiO₃ substrates: a structural study. *J. Phys.: Condens. Matter.* **21**, 182001 (2009).
- Lu, C. L. *et al.* Polarization enhancement and ferroelectric switching enabled by interacting magnetic structures in DyMnO₃ thin films. *Sci. Rep.* **3**, 3374 (2013).
- Ishiwata, S. *et al.* Perovskite manganites hosting versatile multiferroic phases with symmetric and antisymmetric exchange strictions. *Phys. Rev. B* **81**, 100411(R) (2010).
- Lu, C. L. *et al.* Charge-order breaking and ferromagnetism in La_{0.4}Ca_{0.6}MnO₃ nanoparticles. *Appl. Phys. Lett.* **91**, 032502 (2007).
- Zhang, T., Wang, X. P. & Fang, Q. F. Exchange Bias Effect and Suppression of Charge Ordering Induced by a Surface Phase Separation in La_{0.25}Ca_{0.75}MnO₃ Nanowires. *J. Phys. Chem. C* **114**, 11796 (2010).
- Dong, S. *et al.* Surface phase separation in nanosized charge-ordered manganites. *Appl. Phys. Lett.* **90**, 082508 (2007).
- Goto, T., Yamasaki, Y., Watanabe, H., Kimura, T. & Tokura, Y. Anticorrelation between ferromagnetism and ferroelectricity in perovskite manganites. *Phys. Rev. B* **72**, 220403(R) (2005).
- Park, T. J. *et al.* Size-dependent magnetic properties of single-crystalline multiferroic BiFeO₃ nanoparticles. *Nano Lett.* **7**, 766 (2007).
- Nakamura, M., Tokunaga, Y., Kawasaki, M. & Tokura, Y. Multiferroicity in an orthorhombic YMnO₃ single-crystal film. *Appl. Phys. Lett.* **98**, 082902 (2011).
- Zhao, Z. Y. *et al.* Experimental observation of ferrielectricity in multiferroic DyMn₂O₅. *Sci. Rep.* **4**, 3984 (2014).

Acknowledgments

This work is supported by the National Nature Science Foundation of China (Grant Nos. 11104090, 11374112, 11234005, 11374147, 51322206), and the National 973 Projects of China (Grant Nos. 2011CB922101).

Author contributions

J.M.L. and C.L.L. conceived and designed the experiments. X.L. carried out the experiments. J.Y.D. and Y.C. performed the TEM characterization. C.L.L., J.Y.D., S.D. and J.M.L. wrote the paper. X.L., N.H., G.H.W., Z.B.Y. and M.F.L. reviewed and commented on the paper. All the authors discussed the results and commented on the manuscript.

Additional information

Supplementary information accompanies this paper at <http://www.nature.com/scientificreports>

Competing financial interests: The authors declare no competing financial interests.

How to cite this article: Li, X. *et al.* Novel multiferroicity in GdMnO₃ thin films with self-assembled nano-twinning domains. *Sci. Rep.* **4**, 7019; DOI:10.1038/srep07019 (2014).



This work is licensed under a Creative Commons Attribution-NonCommercial-NoDerivs 4.0 International License. The images or other third party material in this article are included in the article's Creative Commons license, unless indicated otherwise in the credit line; if the material is not included under the Creative

Commons license, users will need to obtain permission from the license holder in order to reproduce the material. To view a copy of this license, visit <http://creativecommons.org/licenses/by-nc-nd/4.0/>